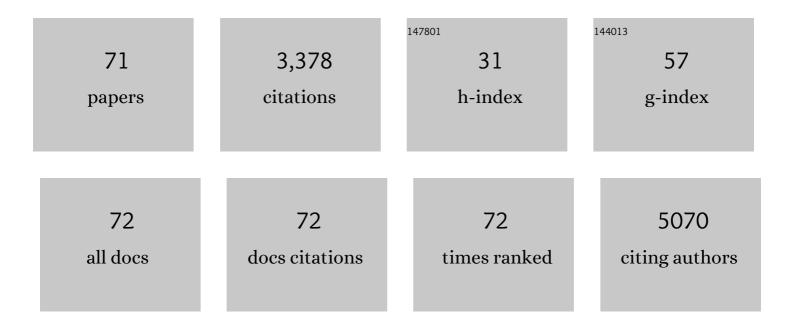
Lidong Sun

List of Publications by Year in descending order

Source: https://exaly.com/author-pdf/8257129/publications.pdf Version: 2024-02-01



#	Article	IF	CITATIONS
1	Electric-field control of magnetism in a few-layered van der Waals ferromagnetic semiconductor. Nature Nanotechnology, 2018, 13, 554-559.	31.5	466
2	Performance improvement of perovskite solar cells through enhanced hole extraction: The role of iodide concentration gradient. Solar Energy Materials and Solar Cells, 2018, 185, 117-123.	6.2	176
3	A green SPEEK/lignin composite membrane with high ion selectivity for vanadium redox flow battery. Journal of Membrane Science, 2019, 572, 110-118.	8.2	153
4	Inverted Planar Perovskite Solar Cells with a High Fill Factor and Negligible Hysteresis by the Dual Effect of NaCl-Doped PEDOT:PSS. ACS Applied Materials & Interfaces, 2017, 9, 43902-43909.	8.0	149
5	Conductivity Enhancement of PEDOT:PSS via Addition of Chloroplatinic Acid and Its Mechanism. Advanced Electronic Materials, 2017, 3, 1700047.	5.1	126
6	High temperature oxidation behavior of hafnium modified NiAl bond coat in EB-PVD thermal barrier coating system. Thin Solid Films, 2008, 516, 5732-5735.	1.8	118
7	Growth of NiMn LDH nanosheet arrays on KCu ₇ S ₄ microwires for hybrid supercapacitors with enhanced electrochemical performance. Journal of Materials Chemistry A, 2017, 5, 20579-20587.	10.3	116
8	Hybrid Membranes Dispersed with Superhydrophilic TiO ₂ Nanotubes Toward Ultraâ€Stable and Highâ€Performance Vanadium Redox Flow Batteries. Advanced Energy Materials, 2020, 10, 1904041.	19.5	115
9	A cost-effective nafion/lignin composite membrane with low vanadium ion permeation for high performance vanadium redox flow battery. Journal of Power Sources, 2021, 482, 229023.	7.8	113
10	The pivotal effects of oxygen vacancy on Bi2MoO6: Promoted visible light photocatalytic activity and reaction mechanism. Chinese Journal of Catalysis, 2019, 40, 647-655.	14.0	86
11	Towards high efficiency thin film solar cells. Progress in Materials Science, 2017, 87, 246-291.	32.8	85
12	Effect of electric field strength on the length of anodized titania nanotube arrays. Journal of Electroanalytical Chemistry, 2009, 637, 6-12.	3.8	79
13	Effect of the Geometry of the Anodized Titania Nanotube Array on the Performance of Dye-Sensitized Solar Cells. Journal of Nanoscience and Nanotechnology, 2010, 10, 4551-4561.	0.9	77
14	Phosphatidylinositol 3-kinase/protein kinase B pathway stabilizes DNA methyltransferase I protein and maintains DNA methylation. Cellular Signalling, 2007, 19, 2255-2263.	3.6	73
15	Highly Stable Vanadium Redoxâ€Flow Battery Assisted by Redoxâ€Mediated Catalysis. Small, 2020, 16, e2003321.	10.0	65
16	Robust Cesium Lead Halide Perovskite Microcubes for Frequency Upconversion Lasing. Advanced Optical Materials, 2017, 5, 1700419.	7.3	64
17	Cuprous sulfide counter electrodes prepared by ion exchange for high-efficiency quantum dot-sensitized solar cells. Journal of Materials Chemistry A, 2014, 2, 2807.	10.3	63
18	A Bi/BiOI/(BiO)2CO3 heterostructure for enhanced photocatalytic NO removal under visible light. Chinese Journal of Catalysis, 2019, 40, 362-370.	14.0	63

LIDONG SUN

#	Article	IF	CITATIONS
19	Biotemplate derived three dimensional nitrogen doped graphene@MnO2 as bifunctional material for supercapacitor and oxygen reduction reaction catalyst. Journal of Colloid and Interface Science, 2019, 544, 155-163.	9.4	63
20	Enhanced photocatalytic activity induced by sp3 to sp2 transition of carbon dopants in BiOCl crystals. Applied Catalysis B: Environmental, 2018, 221, 467-472.	20.2	58
21	Surface Reorganization Leads to Enhanced Photocatalytic Activity in Defective BiOCl. Chemistry of Materials, 2018, 30, 5128-5136.	6.7	55
22	PbS Quantum Dots Embedded in a ZnS Dielectric Matrix for Bulk Heterojunction Solar Cell Applications. Advanced Materials, 2013, 25, 4598-4604.	21.0	50
23	A solar tube: Efficiently converting sunlight into electricity and heat. Nano Energy, 2019, 55, 269-276.	16.0	50
24	SPEEK Membrane of Ultrahigh Stability Enhanced by Functionalized Carbon Nanotubes for Vanadium Redox Flow Battery. Frontiers in Chemistry, 2018, 6, 286.	3.6	49
25	Nanostructured Three-Dimensional Percolative Channels for Separation of Oil-in-Water Emulsions. IScience, 2018, 6, 289-298.	4.1	44
26	Large-Scale, Uniform, and Superhydrophobic Titania Nanotubes at the Inner Surface of 1000 mm Long Titanium Tubes. Journal of Physical Chemistry C, 2017, 121, 15448-15455.	3.1	43
27	A novel parallel configuration of dye-sensitized solar cells with double-sided anodic nanotube arrays. Energy and Environmental Science, 2011, 4, 2240.	30.8	42
28	A Two-step anodization to grow high-aspect-ratio TiO2 nanotubes. Thin Solid Films, 2011, 519, 4694-4698.	1.8	39
29	Fluorinated graphene nanoribbons from unzipped single-walled carbon nanotubes for ultrahigh energy density lithium-fluorinated carbon batteries. Science China Materials, 2021, 64, 1367-1377.	6.3	38
30	Ultralong, Small-Diameter TiO ₂ Nanotubes Achieved by an Optimized Two-Step Anodization for Efficient Dye-Sensitized Solar Cells. ACS Applied Materials & Interfaces, 2014, 6, 1361-1365.	8.0	37
31	Anodic Titania Nanotubes Grown on Titanium Tubular Electrodes. Langmuir, 2014, 30, 2835-2841.	3.5	35
32	A nanopump for low-temperature and efficient solar water evaporation. Journal of Materials Chemistry A, 2019, 7, 24311-24319.	10.3	34
33	Recent advances in photocatalytic decomposition of water and pollutants for sustainable application. Chemosphere, 2021, 276, 130201.	8.2	32
34	Double-Sided Anodic Titania Nanotube Arrays: A Lopsided Growth Process. Langmuir, 2010, 26, 18424-18429.	3.5	30
35	PbS Quantum Dots Capped with Amorphous ZnS for Bulk Heterojunction Solar Cells: The Solvent Effect. ACS Applied Materials & Interfaces, 2014, 6, 14239-14246.	8.0	26
36	Unique lift-off of droplet impact on high temperature nanotube surfaces. Applied Physics Letters, 2017, 111, .	3.3	26

LIDONG SUN

#	Article	IF	CITATIONS
37	Fabrication of TiO ₂ /CuSCN Bulk Heterojunctions by Profile-Controlled Electrodeposition. Journal of the Electrochemical Society, 2012, 159, D323-D327.	2.9	25
38	Nanocomposites of AgInZnS and graphene nanosheets as efficient photocatalysts for hydrogen evolution. Nanoscale, 2015, 7, 18498-18503.	5.6	23
39	Coaxial anodic oxidation under dynamic electrolyte conditions for inner surface patterning of high-aspect-ratio and slim Ti tubes. Corrosion Science, 2017, 124, 193-197.	6.6	22
40	Transition from Anodic Titania Nanotubes to Nanowires: Arising from Nanotube Growth to Application in Dye‧ensitized Solar Cells. ChemPhysChem, 2011, 12, 3634-3641.	2.1	21
41	General Way To Compute the Intrinsic Contact Angle at Tubes. Journal of Physical Chemistry C, 2018, 122, 29210-29219.	3.1	21
42	Ion Selectivity and Stability Enhancement of SPEEK/Lignin Membrane for Vanadium Redox Flow Battery: The Degree of Sulfonation Effect. Frontiers in Chemistry, 2018, 6, 549.	3.6	21
43	Recent developments in slippery liquid-infused porous surface. Progress in Organic Coatings, 2022, 166, 106806.	3.9	21
44	Element diffusion during fabrication of EB-PVD NiAl coating and its 1100°C isothermal oxidation behavior (II). Surface and Coatings Technology, 2007, 201, 6589-6592.	4.8	20
45	Size-dependent crystalline fluctuation and growth mechanism of bismuth nanoparticles under electron beam irradiation. Nanoscale, 2016, 8, 12282-12288.	5.6	19
46	On seeding of the second layer in growth of double-layered TiO2 nanotube arrays. Electrochimica Acta, 2013, 107, 200-208.	5.2	17
47	Interdigitated CuS/TiO2 Nanotube Bulk Heterojunctions Achieved via Ion Exchange. Electrochimica Acta, 2016, 199, 180-186.	5.2	17
48	Effect of Electrolyte Pretreatment on the Formation of TiO ₂ Nanotubes: An Ignored yet Nonâ€negligible Factor. ChemElectroChem, 2018, 5, 1006-1012.	3.4	17
49	The effects of TiO2 nanotubes on the biocompatibility of 3D printed Cu-bearing TC4 alloy. Materials and Design, 2021, 207, 109831.	7.0	17
50	Reversibly tuning the surface state of Ag via the assistance of photocatalysis in Ag/BiOCl. Nanotechnology, 2019, 30, 305601.	2.6	16
51	Conformal Growth of Anodic Nanotubes for Dye-Sensitized Solar Cells: Part I. Planar Electrode. Nanoscience and Nanotechnology Letters, 2012, 4, 471-482.	0.4	16
52	Evolution of Oxyhalide Crystals under Electron Beam Irradiation: An in Situ Method To Understand the Origin of Structural Instability. Inorganic Chemistry, 2018, 57, 8988-8993.	4.0	15
53	Employing ZnS as a capping material for PbS quantum dots and bulk heterojunction solar cells. Science China Materials, 2016, 59, 817-824.	6.3	14
54	Room-temperature up-conversion random lasing from CsPbBr ₃ quantum dots with TiO ₂ nanotubes. Optics Letters, 2019, 44, 4706.	3.3	14

LIDONG SUN

#	Article	IF	CITATIONS
55	Unique dynamics of water-ethanol binary droplets impacting onto a superheated surface with nanotubes. International Journal of Heat and Mass Transfer, 2021, 164, 120571.	4.8	13
56	Conformal Growth of Anodic Nanotubes for Dye-Sensitized Solar Cells: Part II. Nonplanar Electrode. Journal of Nanoscience and Nanotechnology, 2014, 14, 2050-2064.	0.9	12
57	A composite electrode of TiO2 nanotubes and nanoparticles synthesised by hydrothermal treatment for use in dye-sensitized solar cells. RSC Advances, 2013, 3, 11001.	3.6	11
58	Conformal Filling of TiO 2 Nanotubes with Dense M x S y Films for 3D Heterojunctions: The Anion Effect. ChemElectroChem, 2019, 6, 1177-1182.	3.4	10
59	TiO2/CuS core-shell nanorod arrays with aging-induced photoelectric conversion enhancement effect. Electrochemistry Communications, 2020, 111, 106648.	4.7	10
60	Film levitation and central jet of droplet impact on nanotube surface at superheated conditions. Physical Review E, 2020, 102, 043108.	2.1	10
61	Efficient demulsification of ultralow-concentration crude oil-in-water emulsion by three-dimensional superhydrophilic channels. Science China Materials, 2022, 65, 213-219.	6.3	10
62	Three surface modification methods and their effects on the isothermal oxidation behavior of the EB-PVD NiAl coating. Surface and Coatings Technology, 2007, 201, 5161-5164.	4.8	8
63	Alteration of freezing paradigms of an impact water droplet on different cold surfaces. International Journal of Heat and Mass Transfer, 2022, 183, 122177.	4.8	7
64	Dissecting the Chain Length Effect on Separation of Alkane-in-Water Emulsions with Superwetting Microchannels. ACS Applied Materials & Interfaces, 2022, 14, 6157-6166.	8.0	6
65	Towards high-performance transistors and photodetectors with monolayer graphene through modified transfer and lithography process. Materials Express, 2017, 7, 230-236.	0.5	2
66	Polytetrafluoroethylene Modified Nafion Membranes by Magnetron Sputtering for Vanadium Redox Flow Batteries. Coatings, 2022, 12, 378.	2.6	2
67	Conformally anodizing hierarchical structure in a deformed tube towards energy-saving liquid transportation. Chemical Engineering Journal, 2022, 431, 133746.	12.7	1
68	Percolative Anodization: Tailoring TiO ₂ Nanotube Arrays Inside Ultrafine Ti Microchannels. Journal of the Electrochemical Society, 2022, 169, 046517.	2.9	1
69	Anodized Titania Nanotube Array and its Application in Dye-Sensitized Solar Cells. , 2010, , 57-108.		0
70	How to Compute the Contact Angle inside an Opaque Capillary Tube: A Universal Equation. Advanced Theory and Simulations, 0, , 2100474.	2.8	0
71	Recent advances in high-performance membranes for vanadium redox flow battery. , 2022, , 131-154.		0